Live fast and die young

Evolution and fate of massive stars

Renzo, M.

Publication date
2019

Document Version
Other version

License
Other

Massive runaway and walkaway stars

B

B.1 Comparison to selected previous population studies

Various earlier studies have simulated the production of binaries containing a compact object and/or ejecting runaway stars. We briefly discuss a selection that focuses on estimates for unbound companions and comment briefly on how our findings compare.

De Donder et al. (1997) presented an extensive binary evolution study discussing predictions for the O-type runaways as well as the systems that remain bound. They consider a variety of assumptions for the initial distributions and the uncertain physical parameters concerning the efficiency of mass transfer, angular momentum loss and the common envelope ejection. Generally, we find that our results agree well. They find that 16–23% of systems remain bound after the SN explosion of the primary, which is consistent with our findings $1 - \mathcal{D} = 14^{+22}_{-10}\%$. They find that between 6% and 27% of the O-type are unbound former companions that are now single, which is also agreement with our walkaway fraction (one but last column in their table 1).

The find that 2–7% of the O-type stars have velocities large than 30 km s^{-1} (final column in their Table 1), which is slightly larger but still consistent with what we find. We expect that this difference may be in part the result of a difference the treatment of mass transfer and angular momentum loss, although the combined effect of further differences in our assumptions will also contribute. Their default assumption is that a fixed fraction $\beta_{\rm RLOF} = 0.5$ of the material transferred during Roche-lobe overflow leaves the system through the outer L2 Lagrangian point forming a ring around the binary system, which leads to larger angular momentum loss, shrinking the orbit further. This is somewhat similar to our model variation where we assumed $\gamma_{\rm RLOF} = \gamma_{\rm disk}$ although our results cannot be compared one to one, since we adopt a different, physically motivate, assumption for the mass transfer efficiency. In our simulations, we find that this assumption is not increasing the number of runaway stars, because the fraction of system that merges increases too.

Eldridge et al. (2011) perform population synthesis simulations with a detailed stellar evolutionary evolutionary code to investigate O and early B type runaway stars. Their primary aim is the predict the spatial distribution of different types of CCSN and gamma-ray bursts. They find a disruption fraction, $\mathcal{D} = 80\%$, in good agreement with our results, $\mathcal{D} = 86^{+10}_{-22}\%$. In their study, they use the term runaway to refer to all unbound companions with velocities larger than 5km s^{-1}, which encloses the large majority of what we refer to as walkaway

stars, but they also quote estimates for stars faster than 30km s^{-1} which corresponds to our definition of runaway stars. They predict a walkaway (runaway) fraction of 2.2% (0.5%) for O type stars in their simulations for $Z = 0.02$. For comparison, for stars more massive than 15 $M_\odot$, which roughly corresponds to O type stars, we estimate a walkaway (runaway) fraction of $10^{+4.7}_{-8.5}$% ($0.5^{+1.0}_{-0.3}$%). Our runaway fraction agrees very well. We find a somewhat larger walkaway fraction, but we consider this a fairly good agreement, given the uncertainties and differences in definitions that we have adopted. Also the distance they estimate that ejected stars can reach is in good agreement with our predictions and they also note that the majority unbound companions accrete mass from their companions before the first core-collapse. Our predictions for the velocities of bound systems are slightly lower compared to Eldridge et al. (2011): the vast majority of our bound post-core-collapse systems are slower than 30 km s^{-1}, and there is a high-velocity tail barely extending beyond about 100 km s^{-1}.

Very recently, Boubert & Evans (2018) published a study investigating the hypothesis that Be stars are products of mass transfer in binary systems (e.g., Pols et al. 1991; de Mink et al. 2013). They compare the kinematics of a flux-limited sample of Galactic Be stars with binary population synthesis simulations. These simulations were obtained with a different version of the binary evolutionary code that we use. Generally, our findings are in agreement, despite the minor differences in the model assumptions. They also find a large fraction of unbound companions, many of which are rapidly rotating and moving at velocities slower than 30 km s^{-1} (e.g., their Fig. 6 and 7b), in good agreement with our Fig. 3.7. They also find that the natal kick distribution does not greatly affect the resulting velocity distribution and/or the runaway fraction and that the maximum distance traveled by ejected Be stars is likely to be smaller than the vertical scale height of the thin disk, in agreement with our findings.

We find some disagreement in the provided explanations of the theoretical results. For example, the authors state in their section 3.2 that that mass transfer shrinks the orbit and accelerates the secondary star. While this the case initially, upon the onset of mass transfer, we find that the orbit generally widens after the reversal of the mass ratio. The widening and the inversion of the mass ratio both slow down the orbital velocity as we verified both analytically Sec. 3.4 and by detailed inspection of representative example systems, e.g.,Sec. 3.3. In their Section 3.3, they state that "whether a binary is disrupted by a supernova is principally determined by whether the primary loses more than half its mass (Blaauw 1961), and the kick on the compact object is only a second order effect". We find instead that mass loss during the explosion is rarely responsible for unbinding of a binary system that can produce a runaway star. The amount of mass lost needs to exceed half of the total mass of the system (and not half of the primary star), which is rarely achieved in our simulations. This is because the CC progenitor loses most of its mass during the preceding mass transfer phase. We find that the Blaauw kick due to rapid mass loss is only important of initially very wide binaries, in which the two stars have not exchanged mass prior to CC. This difference may be in part due to the differences in the assumptions for the range of initial orbital periods. The authors consider systems with initial orbital periods up to 10^{10} days in their simulations, which means that the majority of their progenitors should effectively evolve as single stars. We consider instead

systems up to $10^{5.5}$ days, which is more appropriate for the more massive progenitors that we are interested in.

Many further studies investigated the populations of binaries in the context of the formation of X-ray binaries and binary neutron stars and black holes. Providing a complete overview and detailed comparison is beyond our present scope. We discuss below a comparison to a limited set of studies.

Brandt & Podsiadlowski (1995) focus on binary systems remaining bound at the first CC, with the aim of understanding the effects of natal kicks on X-ray binaries. They estimate a disruption fraction in their calculations of $\mathcal{D} \simeq 73 - 81\%$ (depending on the companion mass), in good agreement with our results.

Kalogera (1996) presented a similar analytic study of the effects of natal kicks on the systemic velocities of X-ray binaries. Our population synthesis results agree in predicting systemic velocities of bound post-CC systems generally lower than the pre-explosion orbital velocity, except with $\sigma_{\rm kick} \gg v_{\rm orb}^{\rm pre-CC}$ (corresponding to large ξ in the notation used by Kalogera 1996).

Fryer et al. (1998) investigated the impact of NS natal kicks on the formation of NS X-ray binaries and NS-NS binaries, but also present results for the unbound companions. Assuming a bimodal kick distribution, they find that most O/B-type ejected companion move slower than about 50km s^{-1}, consistent with our findings.

Dray et al. (2005) focus on high-mass runaways, which become Wolf-Rayet stars during or before their post-disruption evolution. They argue in favor of significant BH kick amplitudes to explain the rarity of BH-WR binaries and the observed velocity distribution of WR runaways. We reach similar conclusions based on our simulations for different assumptions for the BH kicks. The systemic velocities we find for bound systems are also in reasonable agreement with those found by Dray et al. (2005)

Recently, Tauris et al. (2017) presented a detailed study of the evolutionary processes leading to the formation of NS NS binary systems. They also find that the majority of binaries hosting a NS after the first CC have systemic velocities smaller than $\sim 30\,{\rm km\,s^{-1}}$, in good agreement with the results shown in the left panel of Fig. 3.11.

B.2 Output files

The outcome of our population synthesis calculations will be made available upon publication. For early inquiries, please contact the lead author. Each file corresponds to one parameter variation (see Sec. 3.2 and Sec. 3.6), and logs the following information for each binary system where a star goes CC[1].

- primary ZAMS, pre-CC, and post-CC (corresponding to the NS or BH mass if the primary is the star collapsing) masses in $M_\odot$ units: `M1zams`, `M1preCC`, `M1postCC`;

[1] We stop our computations at the first CC event.

- secondary ZAMS, pre-CC, and post-CC masses in $M_\odot$ units: `M2zams`, `M2preCC`, `M2postCC`;
- fallback fraction f_b for each star (set to zero for the star that is not collapsing): `fb1`, `fb2`
- evolutionary stage before and after CC (stellar types listed according to Hurley et al. 2000): `type1preCC`, `type1postCC`, `type2preCC`, `type2postCC`
- post-CC velocities of the 2 stars in the original frame, in km s^{-1}: `v1postCC`, `v2postCC`;
- pre-CC and post-CC eccentricity (the latter is -1 for mergers and disrupted systems): `e_preCC`, `e_postCC`;
- pre-CC and post-CC separation in $R_\odot$ units (the latter is set to 0 for mergers and disrupted systems): `a_preCC`, `a_postCC`;
- ZAMS, pre-CC, and post-CC periods in days: `Pzams`, `PpreCC`, `PpostCC`;
- kick amplitude in km s^{-1}: `v_kick`;
- kick direction, with θ angle between the collapsing star orbital velocity and the kick (see also TT98 for notation): `theta`, `phi`;
- systemic velocity in km s^{-1}: `v_sys`;
- age of the system at the time of CC in Myr: `t_explosion`;
- time left in the current evolutionary stage in Myr: `t_remaining`;
- time spent by the system with at least one star more massive than 15 $M_\odot$: `duration_*`;
- system probability (see below): `Prob`.

The system probability corresponds to the hyper-volume of the initial parameter space ($M_1^{\rm ZAMS}$, $q^{\rm ZAMS}$, $P^{\rm ZAMS}$) represented by each binary system in our model grid. In other words, the probability of each system is the statistical weight of the system seen as sampling point for the initial distributions. To construct distributions of the output quantities (e.g. those presented in Fig. 3.5-3.11), the properties of each system should be weigh with the corresponding probability. Similarly, the mean value of a quantity $\langle x \rangle$ (e.g. $\langle v \rangle$ in Tab. 3.1) should be calculated using:

$$\langle x \rangle = \frac{\int x P(x)\, dx}{\int P(x)\, dx} \equiv \frac{\sum_i x_i P_i}{\sum_i P_i} \quad , \tag{B.1}$$

where P is the probability, and the index i runs over all the binary systems in a population.

To calculate the average distance traveled by stars ejected by the binary disruption, we use:

$$\langle L \rangle \equiv \langle v \times \Delta t \rangle = \frac{\sum_i \texttt{v2postCC} \times [\texttt{t\_remaining} + 0.1 \times \tau_{\rm MS}(M_2)] \times P_i}{\sum_i P_i} \,, \tag{B.2}$$

where the second term in squared brackets accounts, albeit in a simplified way, for the helium core burning duration of the rejuvenated star.

B.3 Observable velocity distribution

Figure B.1 shows the velocity distribution of MS stars ejected by the disruption of binaries that can be directly compared to observations provided that (i) the contribution of dynamical ejection can be separated in the observed sample and (ii) the effects of the Galactic potential can be neglected, i.e. effectively each ejected star moves in a straight line at constant velocity for the remaining duration of its MS. This is the same information of Fig. 3.5, but each bin is populated considering also the remaining MS lifetime of the ejected star ($\tau_{\rm MS}$).

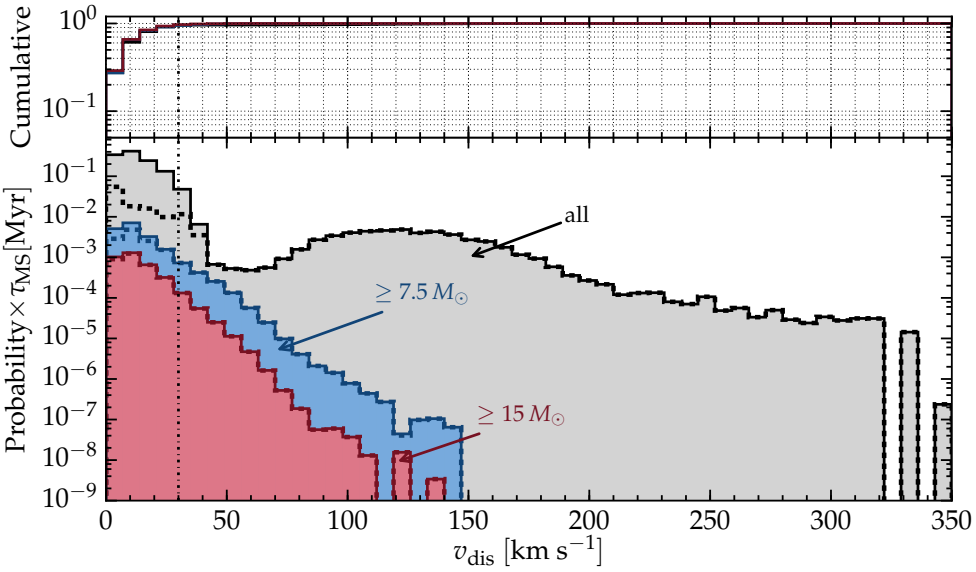

Fig. B.1: Velocity distribution of ejected stars, including the finite MS lifetime to populate the bins (see also Fig. 3.5).

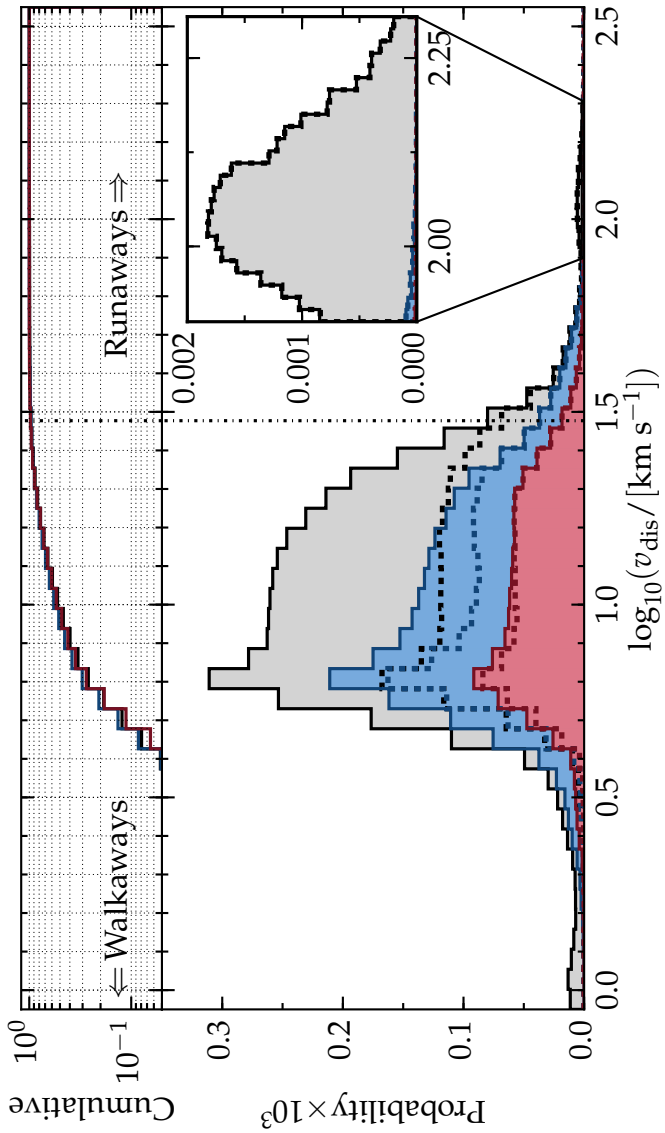

Fig. B.2: Same as Fig. 3.5, but using a logarithmic scale for the velocity. The use of a logarithmic scale allows for the display of a wider range of velocities. A minor peak in the grey histogram can be seen between $100 \lesssim v_{\rm dis}/{\rm km\ s^{-1}} \lesssim 400$, but is absent in the histograms for massive ejected stars. Such high ejection velocities are reached through a common envelope evolution without accreting mass.

B.4 Pre-collapse distributions

We present in this appendix the pre-CC distribution in separation, mass of the collapsing star, and mass of the companions for all the binaries with a MS companion to the collapsing star in our fiducial simulation. Similar distributions can be derived for all our parameter variations from the data files that will be made available.These distributions can inform studies of the interaction of the SN shock with the companion star (e.g., Wheeler et al. 1975; Liu et al. 2015; Rimoldi et al. 2016; Hirai et al. 2018).

We show in Fig. B.3 the pre-CC separation distribution. The colors indicate indicate the minimum mass of the MS companion (i.e., not of the collapsing star). Roughly speaking, the two peaks shown in Fig. B.3 correspond to the orbital widening due to conservative (case A and early case B) and non-conservative (late case B and case C) mass transfer phase. For all pre-CC separations shorter than $10^3\,R_\odot$, the dashed and solid histograms coincide, indicating that all these binaries have experienced a direct interaction previously during the evolution.

Figure B.4 shows the mass distribution for the exploding star and the MS companion ($M_{\rm CC}$, and M_2, respectively), at the pre-CC stage. The combination of the distributions shown in Fig. B.4 and Fig. B.3, together with the effects of the natal kick distribution results in the ejection velocities in Fig. 3.5 which is our main result.

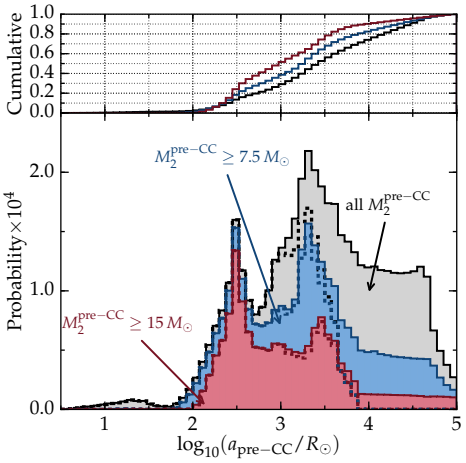

Fig. B.3: Pre-CC separation distribution for binaries with a collapsing star and a main sequence companion. Colors indicate the pre-CC mass of the MS companion according to the legend. Dashed histograms indicate post-interaction (RLOF or common envelope) binaries. The top panel shows the corresponding cumulative distributions.

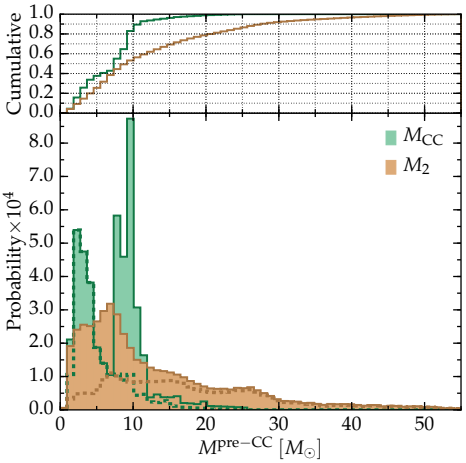

Fig. B.4: Pre-CC mass distribution for the exploding star ($M_{\rm CC}$) and the companion (M_2). We plot all systems where the companion is a MS star at the time of the explosion, regardless of whether the binary is disrupted or not. Dashed histograms indicate post-interaction (RLOF or common envelope) binaries. The top panel shows the corresponding cumulative distributions.